Available online at www.sciencedirect.com
ScienceDirect
Vision Research 47 (2007) 1523–1536
Vision Research
www.elsevier.com/locate/visres

Specific alterations of tyrosine hydroxylase immunopositive cells in the retina of NT-4 knock out mice

Martina Calamusa [a,b], Padmanabhan Paranji Pattabiraman [c], Nikita Pozdeyev [d], P. Michael Iuvone [d], Alessandro Cellerino [b], Luciano Domenici [a,c,e,*]

[a] *Istituto di Neuroscienze, Consiglio Nazionale delle Ricerche (CNR), Via G. Moruzzi 1, 56100 Pisa, Italy*
[b] *Scuola Normale Superiore, 56100 Pisa, Italy*
[c] *Scuola Internazionale Superiore di Studi Avanzati (SISSA), 34014 Trieste, Italy*
[d] *Department of Pharmacology, Emory University, School of Medicine, Atlanta, GA 30322, USA*
[e] *Dipartimento di Scienze e Tecnologie Biomediche, Università di L'Aquila, 67010 L'Aquila, Italy*

Received 6 November 2006; received in revised form 26 January 2007

Abstract

To assess the effect of NT-4 deprivation on maturation of retinal circuitry, we investigated a mouse with targeted deletion of the gene encoding *nt-4* (*nt-4*$^{-/-}$). In particular, we studied neurons immunostained by an antibody recognizing tyrosine hydroxylase (TH), the rate limiting enzyme for dopamine (DA) synthesis. We found that TH immunopositive processes were altered in the retina of *nt-4*$^{-/-}$. Alteration of TH immunopositive processes in *nt-4*$^{-/-}$ mice resulted in changes of DA turnover, as assessed by high-pressure liquid chromatography measurements. These findings suggest that retinal NT-4 plays a role in the morphological maturation of dopaminergic retinal cells.

Keywords: Neurotrophic factors; Visual system; Dopamine; Maturation; *In situ* hybridization

1. Introduction

The expression of neurotrophins has been studied extensively in the central nervous system (CNS), including the visual system (von Bartheld, 1998). BDNF and NT-4 are two neurotrophins expressed in several areas of the CNS that bind to the same TrkB receptor (Barbacid, 1994). The TrkB receptor is expressed by distinct classes of retinal cells (Cellerino & Kohler, 1997; Di Polo, Cheng, Bray, & Aguayo, 2000; Jelsma, Friedman, Berkelaar, Bray, & Aguayo, 1993) and its signalling modulates the retinal response to light (Rohrer, Korenbrot, LaVail, Reichardt, & Xu, 1999; Rohrer, LaVail, Jones, & Reichardt, 2001).

BDNF mRNA and protein are expressed by several subtypes of retinal cells and their expression is activity-dependent (Bennett, Zeiler, & Jones, 1999; Chytrova & Johnson, 2004; Hallbook, Backstrom, Kullander, Ebendal, & Carri, 1996; Herzog, Bailey, & Barde, 1994; Herzog & von Bartheld, 1998; Karlsson & Hallbook, 1998; Perez & Caminos, 1995; Pollock & Frost, 2003; Seki, Nawa, Fukuchi, Abe, & Takei, 2003). BDNF is required for retinal ganglion cell development and function (Alsina, Vu, & Cohen-Cory, 2001; Cellerino, Carroll, Thoenen, & Barde, 1997; Cellerino, Pinzon-Duarte, Carroll, & Kohler, 1998; Cohen-Cory & Fraser, 1995; Du & Poo, 2004; Isenmann, Cellerino, Gravel, & Bahr, 1999; Lom, Cogen, Sanchez, Vu, & Cohen-Cory, 2002; Menna, Cenni, Naska, & Maffei, 2003; Pollock et al., 2003; Rothe, Bahring, Carroll, & Grantyn, 1999), for phenotypic specification of amacrine cells (Cellerino, Arango-Gonzalez, Pinzon-Duarte, & Kohler, 2003; Rickman, 2000), horizontal cells (Pinzon-Duarte, Arango-Gonzalez, Guenther, & Kohler, 2004), bipolar cells

* Corresponding author. Address. Istituto di Neuroscienze, Consiglio Nazionale delle Ricerche (CNR), Via G. Moruzzi 1, 56100 Pisa, Italy.
E-mail address: domenici@in.cnr.it (L. Domenici).

0042-6989/$ - see front matter © 2007 Elsevier Ltd. All rights reserved.
doi:10.1016/j.visres.2007.01.017

(Pinzon-Duarte et al., 2004; Wexler, Berkovich, & Nawy, 1998), and Müller glial cells (Pinzon-Duarte et al., 2004; Wahlin, Campochiaro, Zack, & Adler, 2000).

Dopaminergic amacrine cells are a well-described target of BDNF in the retina. They express TrkB receptors (Cellerino & Kohler, 1997) and are affected in BDNF-deficient mice (Cellerino et al., 1998). Moreover, dopamine release is stimulated by BDNF (Neal, Cunningham, Lever, Pezet, & Malcangio, 2003) and BDNF protects dopaminergic amacrine cells *in vivo* (Seki et al., 2004).

The other TrkB-ligand, NT-4 (Berkemeier et al., 1991; Hallbook, Ibanez, & Persson, 1991), is expressed at low levels in several brain areas (Timmusk, Belluardo, Metsis, & Persson, 1993). Specific and restricted deficits were detected in the CNS of mice with a targeted deletion of *nt-4* gene (*nt-4*$^{-/-}$) (Xie et al., 2000; Roosen et al., 2001; Smith, Leil, & Liu, 2003) demonstrating that low levels of NT-4 have physiological relevance.

Despite the well-known pharmacological effect of exogenous NT-4 upon retinal cells (Cohen, Bray, & Aguayo, 1994; Cui & Harvey, 1994, 1995; Cui & Harvey, 2000; Sawai, Clarke, Kittlerova, Bray, & Aguayo, 1996; Spalding, Cui, & Harvey, 1998; Spalding, Cui, & Harvey, 2005), the role of endogenous NT-4 is still unknown. In addition, evidence that NT-4 is expressed in mammalian retina is lacking.

In the present paper, we investigated whether NT-4 mRNA is expressed in the mouse retina, using RT-PCR and *in situ* hybridization. To assess the effects of NT-4 deprivation on retinal circuitry we analysed a line of null mutant mice with *nt-4* gene deletion (*nt-4*$^{-/-}$). In particular, we focused on the effects of NT-4 deprivation on tyrosine hydroxylase (TH) immunostained retinal cells, which synthesize and release dopamine (for a review see Witkovsky, 2004), express TrkB (Cellerino & Kohler, 1997), and are responsive to BDNF (Cellerino et al., 1998). Potential effects of NT-4 depletion on dopamine retinal content were evaluated by high-pressure liquid chromatography (HPLC). We found that NT-4 is expressed both in developing and adult retina. Its absence induces specific changes in dopaminergic retinal cell morphology and in retinal dopamine turnover.

2. Methods

NT-4 knock out mice (*nt*-4$^{-/-}$; 129S4/SvJae-*Ntf5*^{tm1Jae} strain, Liu, Ernfors, Wu, & Jaenisch, 1995) were obtained from the Jackson Laboratories (Bar Harbor, Maine). Mice with a null mutation of the NT-4 gene are pigmented, viable and fertile and were maintained as a pure homozygous strain. The corresponding 129/Sv strain (Jackson Laboratories, catalog) was used as a wild type control (Fox et al., 2001; Roosen et al., 2001; Smith et al., 2003; Stucky, Shin, & Lewin, 2002; Xie et al., 2000). Animals were kept in a 12 h light/12 h dark cycle, with the illumination level below 60 photopic lux; lights were on from zeitgeber time (ZT) 0-12 and off from ZT 12-24. Mice were genotyped by PCR using genomic DNA isolated from tail biopsies to confirm homozygosity for *nt-4* wild type (WT) and knock out (KO) mice.

Experiments were done in compliance with the Italian laws for the use of animals in research. For euthanasia, adult (2 months) and young mice (postnatal day 15, P15) were anesthetized with an intraperitoneal injection of avertin (1.2% tribromoethanol and 2.4% amylene hydrate in distilled water, 0.1 ml/5 g body weight).

2.1. Retinal RNA extraction and RT-PCR

NT-4 WT (*nt-4*$^{+/+}$, adult mice $n = 4$, P15 mice $n = 4$) mice were anesthetized with avertin, the eyes enucleated, and the retinas isolated. Total RNA from retina was extracted using TriZol (Gibco BRL, Carlsbad, CA). DNase 1 treatment (DNA-free from Ambion Inc, Austin, TX) was carried out according to supplier's instructions to eliminate genomic DNA. Total RNA (5 μg) was used for first strand cDNA synthesis using SUPERSCRIPT reverse transcriptase (Life Technologies Inc, Carlsbad, CA). The cDNA was amplified in a total volume of 50 μl with 1.5 mM $MgCl_2$, 0.2 mM dNTPs, 0.5 μM each of sense and antisense primers for *nt-4*, which yielded a product of 197 bp. A control reaction was done separately with β-actin primers, which yielded a product of 630 bp. The *nt-4* PCR was carried out with a sense primer (5′-TAC TTC TTC gAg ACg Cg-3′) and an antisense primer (5′-AgC TgT gTC gAT CCg AAT CC-3′), first at 94 °C for 3 min, followed by 12 cycles of 94 °C for 20 s, 64 °C for 30 s and 72 °C for 35 s, followed by 25 cycles of 94 °C for 20 s, 58 °C for 30 s and 72 °C for 3 min. The β-actin PCR was performed with a sense primer (5′-CTT TTC ACg gTT ggC CTT Agg gTT-3′) and an antisense primer (5′-AgA TTA CTg CCC Tgg CTC CTA g-3′) at 94 °C for 4 min, followed by 29 cycles of 94 °C for 30 s, 60 °C for 45 s and 72 °C for 10 min. As a negative control, Dnase-treated RNA from retina was screened by PCR with *nt-4* primers to confirm the absence of genomic DNA. This control showed that the PCR product was amplified from cDNA and not from residual genomic DNA in the retinal samples. The RT-PCR products were visualized by agarose gel electrophoresis.

2.2. Riboprobe synthesis

Mouse cDNA obtained from the *nt-4* RT-PCR was gel excised and purified using the QiaQuick purification system. The cDNA was cloned into a pCR II-TOPO vector, and sequenced to check for the correct orientation of the insert and identity to the NT-4 gene sequence. The plasmid (5 μg) was linearized with restriction enzymes and purified with the QiaQuick purification system. Digoxigenen-labeled antisense and sense riboprobes were then synthesized using the respective RNA polymerase (Ambion Inc, Austin, TX) and DIG RNA labeling system (Boeringher, Germany) according to the manufacturer's instruction.

2.3. In situ hybridization

High sensitivity non-radioactive *in situ* hybridization (Pattabiraman et al., 2005; Tongiorgi, Righi, & Cattaneo, 1998) was performed in adult WT mice to check for the retinal layers expressing NT-4 mRNA ($n = 4$ from *nt-4*$^{+/+}$ mice and $n = 4$ from *nt-4*$^{-/-}$ mice). The retinas were harvested in the light phase of the diurnal cycle. Retinal sections of 14 μm thickness were serially sectioned on a cryostat and were washed in PBS 0.1% Tween 20 (PBST). The permeabilization consisted of incubation for 5 min in 2.3% sodium borohydride in 0.1 M Tris–HCl (pH 7.5) followed by 1 mg/ml Proteinase K (Sigma–Aldrich). The time of incubation with Proteinase K was standardized for the various animal groups used. After a wash in PBST, tissue was fixed for 5 min in 4% paraformaldehyde (PFA). Thereafter, prehybridization was carried out at 55 °C for 1 h; incubation with digoxygenin-labeled antisense or sense (control) riboprobe was done overnight at 58 °C followed by post-incubation washes. Immunodetection was done with an anti-DIG antibody F(ab) fragment conjugated to alkaline phosphatase (Roche Biochemicals, Switzerland) at 1:1000 dilution, which was incubated with the sections overnight at 4 °C. Subsequently the sections were washed and developed with NBT/BCIP reaction. An unbiased blind development procedure was used; in particular, reaction was carried out for the same time period for both wild type and the knock out mice in a blind and parallel manner. The reaction was stopped by a stop solution (10 mM Tris–HCl pH 8, 1 mM EDTA) after 35 min for both

nt-4$^{+/+}$ and *nt-4*$^{-/-}$ mice. Sections were washed with PBS, collected onto gelatin-coated slides, cleared with ethanol and xylene and finally mounted with Eukitt mounting medium.

2.4. Enzyme-linked immunosorbent assay (ELISA) for NT-4 and BDNF

Retinas ($n = 4$ from nt-4$^{+/+}$ mice and $n = 4$ from nt-4$^{-/-}$ mice) were extracted and immediately homogenized in 5 volumes of 100 mM Tris buffer (pH 7.4) containing 500 mM NaCl, 2% TritonX-100, 1% NP40, 10% glycerol, and protease and phosphatase inhibitors: 1 mM PMSF, 10 μg/ml aprotinin, 1 μg/ml leupeptin, 0.5 μg/mL antipain, 100 μg/mL benzamidine, 0.1 μg/mL pepstatin A and 0.5 mM sodium vanadate. This homogenate was centrifuged at 14,000 rpm for 30 min and the supernatant fraction was used for ELISA. We performed a sandwich ELISA using the NT-4 and BDNF Emax immunoassay system from Promega (USA) to measure retinal levels of NT-4 and BDNF, respectively. Briefly, 96-well plates were coated with anti-NT4 or anti-BDNF monoclonal antibody and incubated at 4 °C for 18 h. The plates were incubated in a blocking buffer for 1 h at room temperature, then samples were added. The samples, NT-4 and BDNF standards were incubated for 2 h, followed by washing with the appropriate buffer. Successively, the plates were incubated with anti-human NT-4 or anti-human BDNF polyclonal antibody at room temperature for 2 h, washed, and then incubated with specie specific anti-IgG antibody conjugated to horseradish peroxidase for 1 h at room temperature. The plates were finally incubated with chromogen substrate to produce color reaction. The reaction was stopped with 1 M HCl and absorbance was measured at 450 nm using a microplate reader (Model 550, Bio-Rad Laboratories).

The washes were done at least five times in 20 mM Tris–HCl (pH7.6), 150 mM NaCl and 0.05% Tween 20. For each ELISA, the dilutions were such that the NT-4 and BDNF concentrations were within the manufacturer's recommended range.

2.5. DA and DOPAC analysis

Levels of DA and 3,4-dihydroxyphenylacetic acid (DOPAC) in mouse retina were determined by a minor modification of the method of Nir, Haque, and Iuvone (2000). Each retina was homogenized in 70 μl of 0.2 N $HClO_4$ containing 0.01% of sodium metabisulfite and 100 ng/ml of 3,4-dihydroxybenzylamine hydrobromide, an internal standard. After centrifugation at 15,000*g* for 10 min, a 20 μl aliquot of supernatant was analyzed for DA and DOPAC by ion-pair reverse-phase high performance liquid chromatography with amperometric detection (glassy carbon working electrode at 0.65 V vs AgCl reference electrode). The separation was performed on an Ultrasphere ODS 250 × 4.6 mm column, 5 μm (Beckman Coulter, USA) with a mobile phase containing 0.1 M sodium phosphate, 0.1 Mm EDTA, 0.35 Mm sodium octyl sulfate, 5.5% acetonitrile (vol/vol), pH 2.7. External standards of DA and DOPAC were analyzed in each experiment. DA and DOPAC levels were normalized to retinal protein (Lowry, Rosebrough, Farr, & Randall, 1951), using bovine serum albumin as standard.

The levels of dopamine, DOPAC and the ratio DOPAC/dopamine were measured in two groups of adult *nt-4*$^{+/+}$ and two groups of adult *nt-4*$^{-/-}$ mice; in one group, retinas were dissected 1 h after the onset of light in the morning (ZT1) ($n = 3$ from *nt-4*$^{+/+}$ mice and $n = 3$ from *nt-4*$^{-/-}$ mice); in the second group, retinas were dissected at ZT23, 1 h before light onset at the end of the night ($n = 3$ from *nt-4*$^{+/+}$ mice and $n = 3$ from *nt-4*$^{-/-}$ mice). ZT23 retinas were dissected under dim red light. Differences between data from *nt-4*$^{-/-}$ and control mice at ZT1 and ZT23 were evaluated by two way analysis of variance (ANOVA); pairwise comparisons between groups were made using the Student–Newman–Keuls multiple comparison test.

2.6. Histology

Adult and P15 mice, previously anesthetized with an intraperitoneal injection of avertin, were perfused transcardially with 4% paraformaldehyde (PFA) in 0.01 M phosphate buffer, pH 7.4 (PB) in the light phase during the diurnal cycle. The eyes were enucleated, the anterior chamber was removed and the eyecups were fixed for 30 min in the same solution. The fixed eye cups were washed in PB several times and then cryoprotected in 30% sucrose in PB at 4 °C overnight. Eye cups were then embedded in cryomatrix (Tissuetek, Reichart-Jung, Nuβloch, Germany) and frozen. Radial sections (14 μm) were cut on a cryostat (Reichart-Jung, Nuβloch, Germany), collected onto gelatin-coated slides, air-dried, and stored at −20 °C until further processing. Propidium iodide (Molecular Probes, 1:1000 in PBS), a nuclear stain fluorescent in the red spectra, was used to compare the number of rows of photoreceptors in the retina of control and mutant mice.

2.7. Immunocytochemistry

Six *nt-4*$^{+/+}$ and six *nt-4*$^{-/-}$ adult mice and six *nt-4*$^{+/+}$ and six *nt-4*$^{-/-}$ P15 mice were used to perform immunocytochemistry on cryosections. Retinal cross-sections were washed three times in PB and then incubated for 2 h at room temperature in a solution containing 5% bovine albumin (BSA), and 0.3% Triton X-100 in 0.01 M phosphate-buffer at pH 7.4 (PB) (Sigma–Aldrich, St. Louis, MO). Primary and secondary antibodies were diluted in a solution containing 1% BSA and 0.1% Triton X-100 in PB; primary antibodies were applied overnight at 4 °C.

The following primary antibodies were used at the indicated dilutions, determined either from the referenced protocols or from the results of a dilution series: polyclonal anti-protein kinase C (PKC-alpha, Santa Cruz Biotechnology, Inc., Santa Cruz, CA; 1:1000 after run dilution series), a marker for rod-bipolar cells; monoclonal anti-calbindin-D28K (Sigma–Aldrich, St. Louis, MO; 1:1000; Pignatelli, Cepko, & Strettoi, 2004), a marker for horizontal cells; polyclonal anti-disabled-1, a marker for AII amacrine cells (DB-1, a kind gift of D. Rice, Memphis, USA; 1:1000 after run dilution series); polyclonal anti-tyrosine hydroxylase (TH, Chemicon, Temecula, CA; 1:500 after run dilution series), a marker for dopaminergic amacrine cells (Witkovsky et al., 2004); polyclonal anti-parvalbumin (Swant, Switzerland; 1:1000; Pignatelli & Strettoi, 2004), a marker for mouse retinal ganglion cells (Kim & Jeon, 2006).

Secondary antibodies, conjugated to Alexa 488 (Molecular Probes, Eugene, OR; 1:400), were applied for 2 h at room temperature. Sections were washed three times in PB and then coverslipped with Vectashield (Vector laboratories, Burlingame, CA). To control for the specificity of the antibodies, parallel experiments with omitted primary antibody were performed in control and mutant mice.

For whole mount immunostaining experiments, retinas were separated from the pigment epithelium and four radial cuts were made to allow them to flatten. The retinas were then post fixed in 4% paraformaldehyde for 30 min. Samples were rinsed in 0.01 M phosphate buffer at pH 7.4 (PB) for 15 min and put in blocking solution (5% BSA, 0,3% Triton X-100 in PB) overnight at 4 °C. Retinas were incubated with antibody solution (polyclonal anti-tyrosine hydroxylase TH, Chemicon, 1:200, 1% BSA, 0,1% Triton X-100 in PB) and left at 4 °C for five days, washed several times in PB, and placed for 2–3 days in the secondary antibody solution (anti-rabbit Alexa 488, 1% BSA, 0,1% Triton X-100 in PB) to reveal immunoreactive cells.

2.8. Quantification of TH immunopositive cell bodies and varicosities in whole mount retina

Counts of TH immunopositive cell bodies and varicosities were made from whole mount retina of *nt-4*$^{+/+}$ ($n = 4$) and *nt-4*$^{-/-}$ ($n = 4$) mice using a fluorescence Nikon microscope with a Plan-Four 4×/0.13 objective. Each retina was subdivided randomly in four quadrants. We acquired and printed one image for each retinal quadrant from which the entire retinal surface was reconstructed. Each dopaminergic cell was counted from the prints. The size of the whole retina was measured with Metamorph® software in adult mutant ($n = 4$) and control mice ($n = 4$) after acquisition of four retinal quadrants with the fluorescence microscope.

For quantification of TH immunopositive varicosities, each retinal quadrant was further subdivided in 3 fields of acquisition: one peripheral, one mid-peripheral and one central (5/6, 3/6 and 1/6 of retinal radius). For each field, serial optical sections were acquired using a Leica TCS-NT confocal microscope equipped with a krypton-argon laser and high resolution

images (1024 × 1024 pixels) were obtained using Plan-Apocromatic 40×/1.0 objective. The optical sections were 1 μm apart and they covered the total thickness of the TH immunopositive network, localized in the inner plexiform layer (IPL). Given an optical *z*-resolution of ~0.7 μm, and the fact that almost no varicosities are confined to a single *z*-plane, this spacing was selected to minimize chances of over-sampling or undersampling.

In whole mount retina, the TH immunopositive processes contained two classes of varicosities: one class is organized into pericellular rings surrounding the *somas* of AII amacrine cells (Kolb, Cuenca, Wang, & Dekorver, 1990), and another class containing all the varicosities not contacting the cell bodies of these amacrine cells (non-AII varicosities). The numbers of these two types of dopaminergic varicosities were quantified by dividing each 252 × 252 μm image, representing a single optical section in a Z-stack, into 144 squares of 21 × 21 μm. By using a random number table, we selected the squares to be analysed, and counted the number of varicosities forming each of six different rings, expressing the final count as the mean number of varicosities/ring averaged over a total of 288 randomly selected rings in 48 different optical sections from four different mice for each genotype. We also counted the number of rings in six different frames using the same sampling method. A sample size of six provides sufficient statistical power to accurately determine the average number of varicosities per ring and assess whether there is a statistically significant difference between WT and KO mice in this parameter.

Finally, in two different frames randomly sampled we counted the number of non-AII varicosities (see Fig. 5B and C). Differences between the data obtained in *nt-4*$^{+/+}$ and *nt-4*$^{-/-}$ mice were tested statistically with the Student's *t* test.

2.9. Quantification of TH stained areas in cross-sections of retina

The retinal TH stained areas in the IPL and in the outer plexiform layer (OPL) of *nt-4*$^{-/-}$ P15 mice ($n = 6$), *nt-4*$^{+/+}$ P15 mice ($n = 6$), *nt-4*$^{-/-}$ adult mice ($n = 6$), and *nt-4*$^{+/+}$ adult mice ($n = 6$) were quantified using Metamorph® software (Universal Imaging Corp.). TH stained retinal sections were acquired using a confocal microscope. For each animal, 3 Z-stack of serial images were acquired and for each of these, an area of fixed size was selected within the OPL and the IPL. The number of pixels above a fixed threshold of brightness was calculated within the selected areas. The threshold of brightness, the same for every Z-stack of serial images analyzed, was chosen to eliminate the nonspecific background signal in immunostained TH retinal sections; to this aim, at first we evaluated the mean variation in background for each mouse and then we utilized a threshold well over the mean noise level. Since the distribution of pixels over threshold was non-Gaussian, we used the Wilkoxon–Mann Whitney *U*-test (Statistica, Statsoft) to test for statistical differences. Quantification of TH immunostained processes in the retina of *nt-4*$^{+/+}$ and *nt-4*$^{-/-}$ mice was performed blind.

3. Results

3.1. NT-4 is expressed in the adult and P15 retina of wild type mouse

We carried out RT-PCR experiments on retinal RNA obtained from *nt-4*$^{+/+}$ adult and P15 mice with primers designed from the coding region of the *nt-4* gene. A specific band of approximately 200 bp was amplified (Fig. 1) in adult and P15 WT mice while it was absent in *nt-4*$^{-/-}$ adult and P15 mice. To control for genomic DNA contamination, *nt-4* PCR was performed on retinal RNA not treated with reverse transcriptase; no PCR product was detected in these samples (-RT in Fig. 1A). In addition, we detected expression of NT-4 protein in the retina of wild type mice using enzyme-linked immunosorbent assay (ELISA, see Section 2 and previous report by Fan et al., 2000). NT-4 was found to be expressed without significant changes of the protein level between P15 and adult retinas. No signal was detected in homogenates from *nt-4*$^{-/-}$ mice retinas (Fig. 1C).

To localise retinal cells expressing NT-4 mRNA, we performed non-radioactive *in situ* hybridization (Pattabiraman et al., 2005; Tongiorgi et al., 1998) on retinal cross-sections of *nt-4*$^{+/+}$ and *nt-4*$^{-/-}$ adult mice. Positive staining was

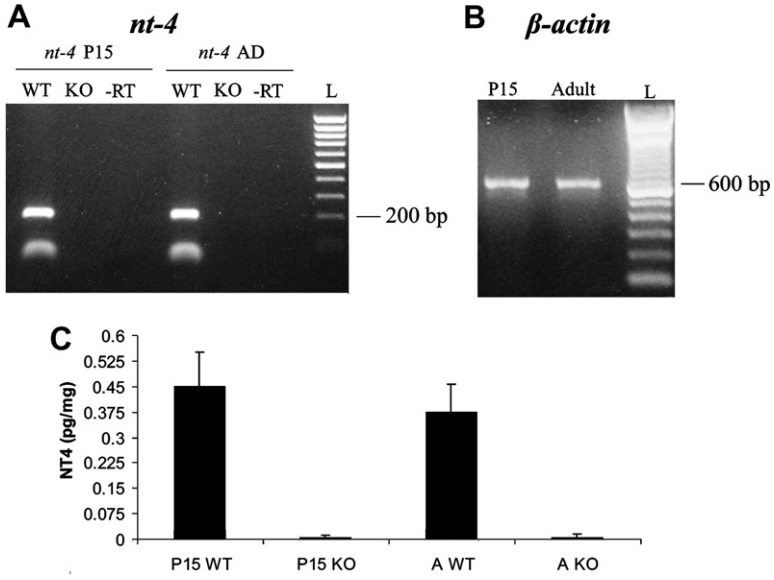

Fig. 1. NT-4 RT-PCR in the retina from adult and P15 wild type mice. (A) A band of about 200 bp, corresponding to a partial NT-4 transcript, was amplified from retinal RNA of *nt-4*$^{+/+}$ P15 and adult mice (WT); the amplicon was absent in *nt-4*$^{-/-}$ samples (KO). To control for genomic DNA contamination, PCR was performed on retinal RNA not treated with reverse transcriptase (see -RT lanes, *nt-4* P15 and *nt-4* AD). AD means adult. (B) Positive control RT- PCR for β-actin mRNA. (C) NT-4 protein level (pg/mg tissue) was determined by ELISA. NT-4 was detected in retina of *nt-4*$^{+/+}$ but not *nt-4*$^{-/-}$ mice. The difference between P15 and adult level of NT-4 in WT mice (P15 WT and A WT, respectively) was not statistically significant.

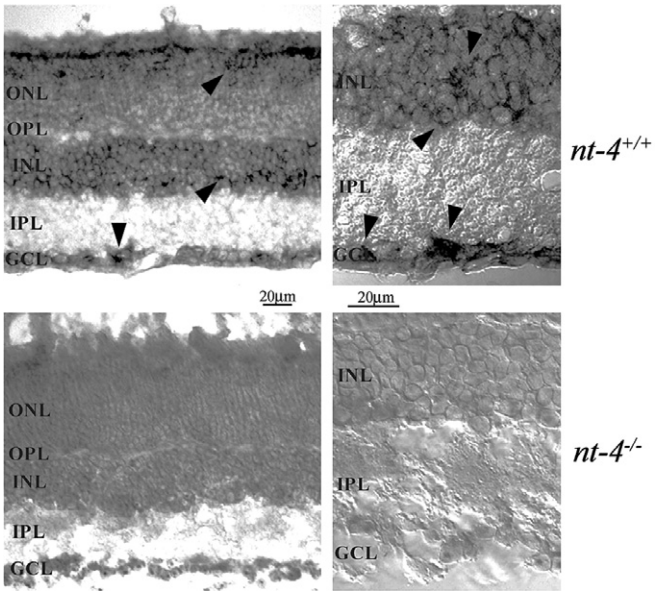

Fig. 2. *In situ* hybridization on retinal cross-sections of *nt-4*$^{+/+}$ and *nt-4*$^{-/-}$ mice. (Top row) In the retina of adult *nt-4*$^{+/+}$ mice, the staining was localized in cells of the ONL, INL and GCL (see arrowheads). (Bottom row). The retinal cross-sections of adult *nt-4*$^{-/-}$ mice showed diffuse, non-specific staining throughout all retinal layers. *Abbreviations:* ONL, outer nuclear layer; OPL, outer plexiform layer; INL, inner nuclear layer; IPL, inner plexiform layer; GCL, ganglion cell layer. Scale bars are reported between top and bottom row.

observed in retinas of *nt-4*$^{+/+}$ mice (Fig. 2) and was localised to the cells of the inner nuclear layer (INL), to the outer nuclear layer (ONL) and in a few cells of the ganglion cell layer (GCL). Although the level of hybridization is clearly lower in the ONL than in the INL, the reaction product in these two retinal layers appears to be distributed in rings that outline the soma or nucleus. The only solidly labeled cells are in the retinal ganglion cell layer. In particular, the hybridization signal in the most inner part of INL of *wild type* mice localized to a spatial position typical for amacrine cells. The retinal sections of *nt-4*$^{-/-}$ mice lacked localised staining in any retinal layer (Fig. 2).

Further control for specificity was performed using a sense riboprobe on wild type retinas; in this experimental condition no signal was detected (data not shown). Thus, the *nt-4* gene is actively transcribed in retina, mainly in cells in the INL and GCL.

3.2. Tyrosine hydroxylase immunocytochemical analysis of the retina of *nt-4*$^{-/-}$ mice

We performed immunocytochemistry on cross-sections of *nt-4*$^{+/+}$ and *nt-4*$^{-/-}$ mouse retina using an antibody recognizing tyrosine hydroxylase (TH), the rate limiting enzyme for dopamine synthesis. The somata of TH immunostained amacrine cells are found in the innermost part of the INL (Fig. 3) and a network of TH-immunoreactive processes is localized in stratum 1 (S1) of IPL, in accordance with previous data on the retinal dopaminergic network (Cellerino et al., 1998; Dacey, 1990; Voigt & Wassle, 1987; for a review see Witkovsky, 2004). In addition, this retinal cell expresses TrkB (Cellerino & Kohler, 1997) and, thus, is potentially sensitive to NT-4. TH immunocytochemistry on retinal cross-sections of *nt-4*$^{-/-}$ adult mice revealed differences with respect to *nt-4*$^{+/+}$ mice. Some of these TH immunopositive cells extend ascending processes towards the OPL. In *nt-4*$^{-/-}$ adult mouse, these ascending processes appeared more widespread than in *nt-4*$^{+/+}$ mice, occupying a greater retinal area, particularly in the OPL (Fig. 3, see A and B, see also quantitative results in Fig. 4).

At P15, TH immunopositive retinal cells are not yet fully mature (Wulle & Schnitzer, 1989) and, therefore, this postnatal age represents a developmental stage of active

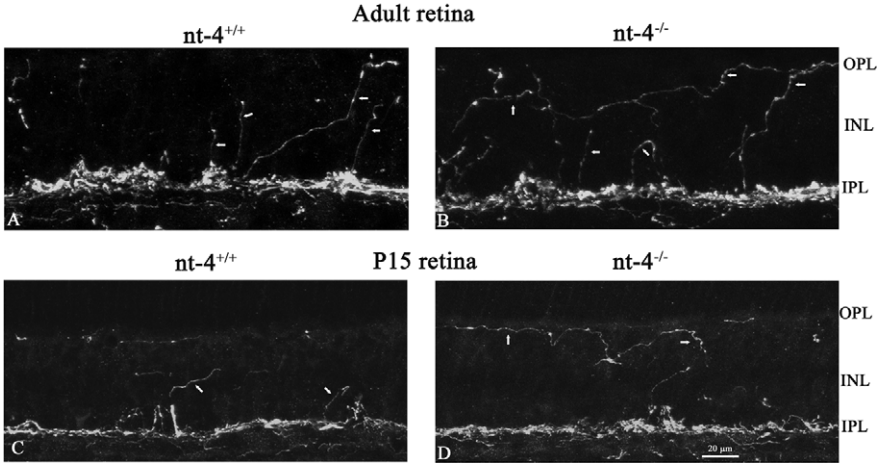

Fig. 3. TH immunocytochemistry in *nt-4*$^{+/+}$ and *nt-4*$^{-/-}$ adult and P15 retinal sections. Immunocytochemistry in radial sections of retinas with TH antibody identifies not only the dopaminergic network that is localized at the border between INL and IPL, but also the processes that ascend towards the OPL. Adult retinas are illustrated in (A) and (B); P15 retinas are shown in (C) and (D). The TH-immunopositive cell bodies are not shown in the images. The spread of dopaminergic ascending processes in retinal sections of *nt-4*$^{-/-}$ (B) was increased compared to that in control retinal sections of *nt-4*$^{+/+}$ adult mice (A). Similarly, the spread of the ascending processes was greater in retinas of *nt-4*$^{-/-}$ mice (D) than in those of *nt-4*$^{+/+}$ mice (C) at P15. Also, the dopaminergic plexus in the IPL of P15 *nt-4*$^{-/-}$ mice (D) was increased with respect to that in age-matched *nt-4*$^{+/+}$ mice (C). Scale bar (20 μm) is reported in (D).

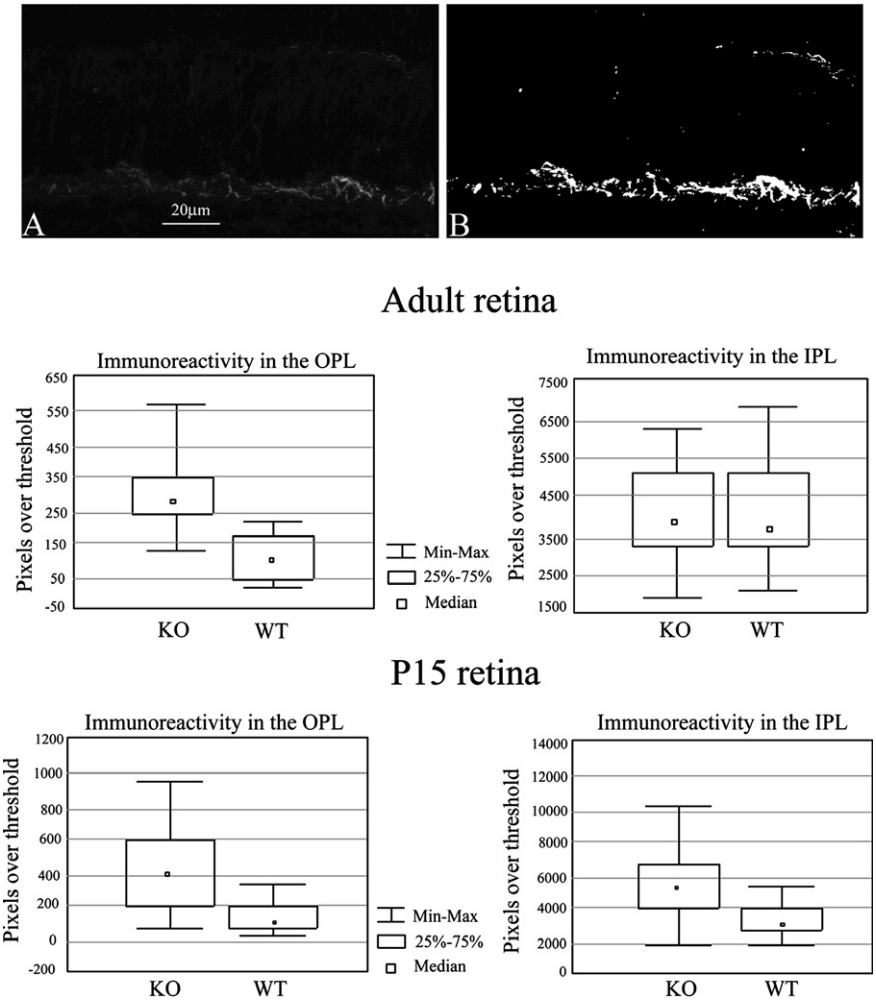

Fig. 4. Quantification of TH process spread in retinas of *nt-4*$^{-/-}$ and *nt-4*$^{+/+}$ mice. The image in (A) shows mouse retinal section acquired using a confocal microscope with low, non saturating intensity; the image in (B) shows the same retinal section as in (A), following the application of a brightness threshold. For each image, two areas of fixed size were selected in the OPL and IPL. The white pixels within rectangles and over fixed threshold were counted using Metamorph® software. The distributions of pixels over threshold in the OPL and in the IPL of *nt-4*$^{+/+}$ (WT) and *nt-4*$^{-/-}$(KO) mice in adulthood and at P15, are presented in the histograms. Quantitative analysis of TH immunoreactivity performed in the IPL of adult mice (adult retina) did not reveal significant differences between *nt-4*$^{+/+}$ and *nt-4*$^{-/-}$ mice; in contrast, a significant increase in the area occupied by dopaminergic ascending fibers was present in the OPL of *nt-4*$^{-/-}$ adult mice (*U*-test, $p = 0.003$). In P15 retina of *nt-4*$^{-/-}$ mice, the morphometric analysis of TH immunoreactivity revealed a 74% increase in the area occupied by dopaminergic network in the IPL (*U*-test, $p = 0.05$) and a 281% increase in the area occupied by dopaminergic ascending fibers in the OPL (*U*-test, $p = 0.004$) compared to *nt-4*$^{+/+}$ mice. In the graphics the dots represent median values, the boxes represent the 25–75% percentile intervals and the bars represent minimum and maximum values. The analysis was performed on *nt-4*$^{-/-}$ ($n = 6$) and *nt-4*$^{+/+}$ ($n = 6$) at P15, and on *nt-4*$^{-/-}$ ($n = 6$) and *nt-4*$^{+/+}$ ($n = 6$) adult mice.

morphological growth of dopaminergic connections; this is particularly true of dopaminergic processes, whose growth during the 3rd postnatal week was documented by Witkovsky, Arango-Gonzalez, Haycock, and Kohler (2005). TH immunocytochemistry performed on retinal sections of P15 *nt-4*$^{+/+}$ and *nt-4*$^{-/-}$ mice revealed a distribution of ascending dopaminergic processes in *nt-4*$^{-/-}$ mice, similar to what is observed in adult mice. In addition, P15 *nt-4*$^{-/-}$ mice showed an increase in the thickness of dopaminergic network localised in the IPL (Fig. 3, compare C, D). Thus, the absence of NT-4 affects the maturation of the dopaminergic phenotype in the mouse retina.

The areas occupied by dopaminergic fibers in the OPL and IPL were quantified by counting pixels over a fixed threshold of brightness within windows of standardized size (see Section 2). The distribution of pixel number over threshold in the OPL and in the IPL of *nt-4*$^{+/+}$ and *nt-4*$^{-/-}$ adult and P15 mice is illustrated in Fig. 4. In adult mice, significant differences between *nt-4*$^{+/+}$ ($n = 6$) and *nt-4*$^{-/-}$ ($n = 6$) genotypes were found in the OPL only; in mutant mice, the area of the OPL occupied by dopaminergic fibers was 2.5 times that of *nt-4*$^{+/+}$ (*U*-test, $p = 0.003$). Analysis of P15 mouse retinas revealed a 281% increase in the OPL in *nt-4*$^{-/-}$ ($n = 6$) compared to *nt-4*$^{+/+}$ ($n = 6$) mice (*U*-test, $p = 0.004$). In addition, the area occupied by the dopaminergic processes in the IPL of P15 *nt-4*$^{-/-}$ mice was 1.2 times higher than that of age-matched *nt-4*$^{+/+}$ controls (*U*-test, $p = 0.05$).

The result showing that TH immunopositive processes were apparently unaffected in adult IPL of mutant mice prompted us to investigate the dopaminergic circuitry of the IPL in more detail. We examined the varicosities distributed along the TH immunopositive processes. Different types of TH varicosities have been previously described in dopaminergic cells (Kolb et al., 1990). One type organizes into pericellular rings (Tork & Stone, 1979) surrounding the cell bodies of AII amacrine cells. Also A17 amacrine cells may present dopaminergic varicosities around their soma that often appear as half ring; both types of varicosities belong to the rod pathway (Bloomfield & Dacheux, 2001; Famiglietti & Kolb, 1975; Voigt & Wassle, 1987). Another type includes all the varicosities not contacting somas of AII and other amacrine cells (non-AII varicosities). In analysed mouse retinas, we found dopaminergic non-AII varicosities and dopaminergic varicosities forming pericellular rings, thus likely to be on AII amacrine cells (Fig. 5A). Non-AII TH immunopositive varicosities showed a 20% increase in *nt-4*$^{-/-}$ retina (Mean = 53, *SD* = 2,9, *n* = 4) relative to *nt-4*$^{+/+}$ (Mean = 44,5, *SD* = 4,8, *n* = 4) retina (Fig. 5B, *t*-test, $p < 0.01$). This result was specific, since neither the varicosities forming a typical ring around the cell bodies of AII amacrine cells nor the number of rings was different between genotypes (Fig. 5C). In addition we found that the number of TH stained cell bodies was not significantly different between *nt-4*$^{-/-}$ (Mean = 611, *SD* = 76, *n* = 4) and *nt-4*$^{+/+}$ mice (Mean = 588, *SD* = 115, *n* = 4) (Fig. 6C). To exclude non specific effects due to changes of retinal size, we measured the total area in whole

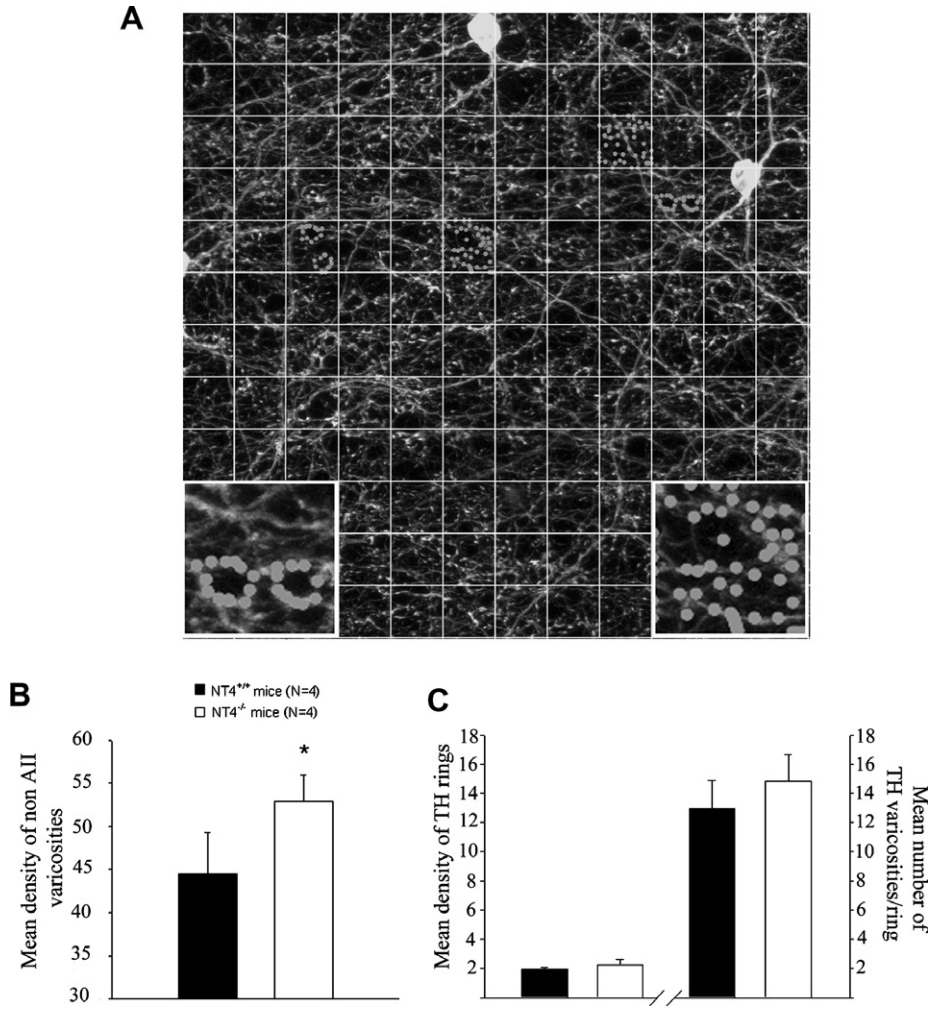

Fig. 5. Non-AII varicosities are affected in the retina of *nt-4*$^{-/-}$ mice. (A) Illustration of the method used to count the TH immunopositive varicosities in whole mount retina. One retinal field was acquired using a confocal microscope. The number of two types of TH immunostained varicosities (pericellular rings and non-AII varicosities) present in the image was measured superimposing a grid made of 21 × 21 μm frames (12 × 12 matrix). These varicosities were counted in quadrants randomly sampled (see Section 2). Each varicosity was marked after counting to avoid recounting. Higher magnifications of two frames in the left and right bottom corner represent pericellular rings (left side) and non-AII varicosities, (right side), respectively, after counting and marking. (B) Histogram. The number of TH immunostained non-AII varicosities showed a 20% increase in *nt-4*$^{-/-}$ over those present in *nt-4*$^{+/+}$ retina (*, *t*-test, $p < 0.01$). The analysis was performed on mutant (*n* = 4) and control mice (*n* = 4). Columns represent the means (*SD* is represented as vertical bar). (C) Histogram. On the left side, the mean density of TH rings and on the right side, the mean number of TH varicosities per ring are shown. There is no difference between control (*n* = 4) and mutant (*n* = 4) mice. Columns represent the means (*SD* is represented as vertical bar).

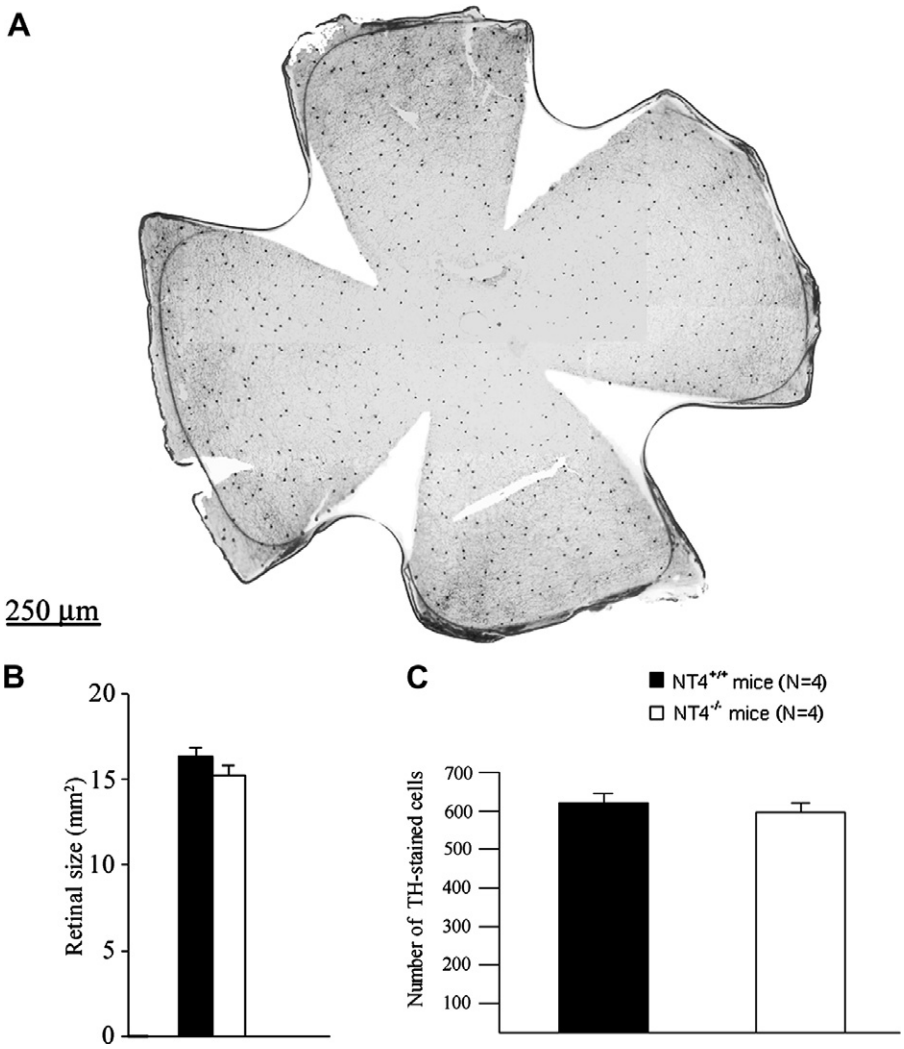

Fig. 6. The number of TH immunopositive cell bodies is unchanged in the retina of *nt-4*$^{-/-}$ mice. (A) Dopaminergic cell bodies were stained in whole mount retina of *nt-4*$^{+/+}$ ($n=4$) and *nt-4*$^{-/-}$ ($n=4$) mice; we illustrate an example of retina stained with TH antibody. Scale bar = 250 µm. (B) The analysis of retinal size performed on the retina of four *nt-4*$^{+/+}$ and four *nt-4*$^{-/-}$ revealed no statistically significant difference. Columns represent the means (*SD* is represented as vertical bar). (C) Histogram. The number of TH stained cell bodies was not significantly different between *nt-4*$^{-/-}$ (Mean = 611, *SD* = 76) and *nt-4*$^{+/+}$ (Mean = 588, *SD* = 115).

mount retinas in adulthood: we found no significant differences between mutant and control mice (Fig. 6B). These results indicate that in *nt-4*$^{-/-}$ mice there is an increase in dopaminergic varicosities that is specifically directed to non-AII targets.

In order to determine whether an increased spread of TH immunopositive processes and a high number of TH varicosities is associated with a change of dopamine synthesis and/or turnover, we measured the steady-state levels of DA and its metabolite DOPAC during the night (1 h before lights on, ZT23) and in light, 1 h into the day (ZT1). There were no significant differences in steady state DA level between *nt-4*$^{+/+}$ and *nt-4*$^{-/-}$ mice (Fig. 7A). To ascertain whether dopamine turnover was altered in the absence of NT-4, the ratio DOPAC/DA was calculated. In agreement with previous reports (e.g. Nir et al., 2000), the DOPAC/DA ratio increased 1 h after light onset in the morning in both mutant and control mice (Student–Newman–Keuls test $p<0.01$; Fig. 7C). No significant differences in the DOPAC/DA ratio were found between *nt-4*$^{+/+}$ and *nt-4*$^{-/-}$ mice in darkness. However, the DOPAC/DA ratio 1 h after light onset was ~30% higher in *nt-4*$^{-/-}$ mice compared with *nt-4*$^{+/+}$ controls (Student–Newman–Keuls test $p<0.01$; Fig. 7C). Thus, a higher level of light-evoked DA turnover in retinae of *nt-4*$^{-/-}$ mice correlates with the larger number of non-AII TH positive varicosities and the increased spread of dopaminergic fibers.

We next examined whether the altered retinal TH immunopositive neurons in mutant mice were associated with changes of BDNF protein, the other member of neurotrophin family that binds to TrkB. Examination of BDNF by ELISA revealed a normal level in the retina of mutant mice (*nt-4*$^{+/+}$ mice, $n=4$, 67 ± 41 pg/mg protein; *nt-4*$^{-/-}$ mice, $n=4$, 67 ± 21 pg/mg protein, data not shown). These data indicate that alteration of TH immunopositive retinal cells in *nt4*$^{-/-}$ mice is not due to a compensatory up-regulation of BDNF level.

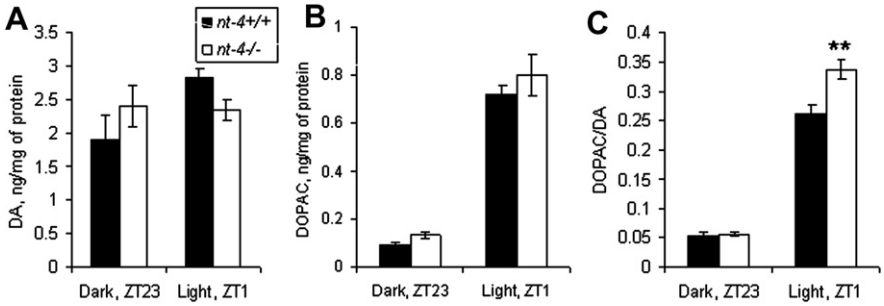

Fig. 7. Dopamine and DOPAC levels in the retina of *nt-4*$^{+/+}$ and *nt-4*$^{-/-}$ mice. The steady-state levels and turnover of DA were evaluated in two groups of adult *nt-4*$^{+/+}$ and two groups of adult *nt-4*$^{-/-}$ mice; one group was dissected 1 h after light onset (ZT1) and the other dissected 1 h before light onset (ZT23). For each group, 6 pairs of retinas were used at ZT1 and 6 pairs at ZT23. Levels of DA and DOPAC, the main DA metabolite, in mouse retina were determined by high-pressure liquid chromatography (HPLC). (A) There are no significant effects of genotype or light exposure on DA levels. (B) Light exposure significantly increased DOPAC levels ($p < 0.001$) with no significant effect of genotype. (C) The DOPAC/DA ratio, an index of DA turnover, was significantly increased by light exposure in both genotypes ($p < 0.001$); there was a significant effect of genotype ($p < 0.05$) and a significant interaction of lighting condition and genotype ($p < 0.05$). The DOPAC/DA ratio was higher in *nt-4*$^{-/-}$ mice compared to *nt-4*$^{+/+}$ mice at ZT1 in light (**$p < 0.01$), but not in darkness at ZT23 ($p = 0.883$).

Finally, we analysed the effects induced by NT-4 depletion on other retinal cell subtypes in order to exclude gross impairment of retinal circuitry. To this aim we used the following specific markers of retinal cells: protein kinase C (marker for rod bipolar cells), calbindin (marker for horizontal cells), disabled-1 (marker for AII amacrine cells), and parvalbumin (marker for mouse ganglion cells, Kim & Jeon, 2006). In addition, we examined photoreceptors using propidium iodide as a marker. Lack of *nt-4* gene did not grossly affect the maturation of photoreceptors, rod bipolar, horizontal, AII amacrine and ganglion cells, as illustrated in Fig. 8.

4. Discussion

In the present paper, we report that both NT-4 mRNA and protein are expressed in the wild type mouse retina. NT-4 absence in NT-4 knockout mice is associated with an abnormal maturation of TH immunostained retinal cells.

We showed the presence of NT-4 mRNA using RT-PCR and *in situ* hybridization. NT-4 mRNA is expressed in several cells of different retinal layers but it is most concentrated in the INL and, particularly, in cells that have the location of amacrine cells. This result suggests that expression of NT-4 mRNA is particularly relevant in the inner retina and supports a possible direct action of NT-4 on amacrine cells. Concerning the NT-4 protein measurement, although this measurement is difficult to interpret due to protein trafficking between the retina and its targets (for a review see Frost, 2001), our data indicate that NT-4 protein is expressed at low level both during postnatal development (P15) and in adult mouse retina.

To investigate whether NT-4 deprivation affects maturation of retinal circuitry in the mouse retina, we analysed the phenotype of retinal cells in null mutant mice devoid of *nt-4* gene. *Nt-4*$^{-/-}$ mice are the only strain of neurotrophin knock out whose homozygous mutants are viable. Detailed analysis of these mice revealed restricted and peripheral alterations at both anatomical and functional levels (Conover et al., 1995; Erickson et al., 1996; Fox et al., 2001; Liu et al., 1995; Lucas et al., 2003; Roosen et al., 2001; Smith et al., 2003; Stucky et al., 2002; Xie et al., 2000).

Our results showed that the absence of NT-4 targets TH immunopositive cells, while several other retinal neurons do not appear to be grossly affected. Lack of NT-4 causes a general alteration of these cells, as shown using immunocytochemistry for TH. In particular, our results revealed an increase of the retinal area occupied by the TH immunopositive network, which in P15 mice involves ascending dopaminergic processes in OPL and the dopaminergic plexus localized in IPL, whereas in adult the alterations are restricted to the OPL.

Dopamine is the primary catecholamine neurotransmitter synthesized in the retina of most vertebrate species (Iuvone, 1986), and the TH immunopositive amacrine cells are generally considered to be dopaminergic (Witkovsky et al., 2004). The morphology of these cells in mammalian retina is well-described (for a review see Witkovsky, 2004) and at least different sites of dopamine release can be clearly differentiated: varicosities organized into pericellular rings, which specifically target AII amacrine cells (Bloomfield & Dacheux, 2001; Kolb et al., 1990) and varicosities not contacting these particular neurons. As only the latter is affected in *nt*-4$^{-/-}$ mice we conclude that absence of NT-4 specifically affects a defined subset of varicosities not associated with the rings. It must be noted that even if these varicosities are not adjacent to a particular cell type, the dopamine released there may ultimately affect them by diffusion (for review see Witkovsky et al., 2004). Diffusion distances of dopamine can be small—less than 1 μm—or very great—tens of microns, in this way affecting many retinal cells expressing dopamine receptors.

The greater spread of TH immunopositive processes and higher number of varicosities in retinas of *nt-4*$^{-/-}$ mice was expected to affect DA content and metabolism. We investigated diurnal variations in the levels of DA and its

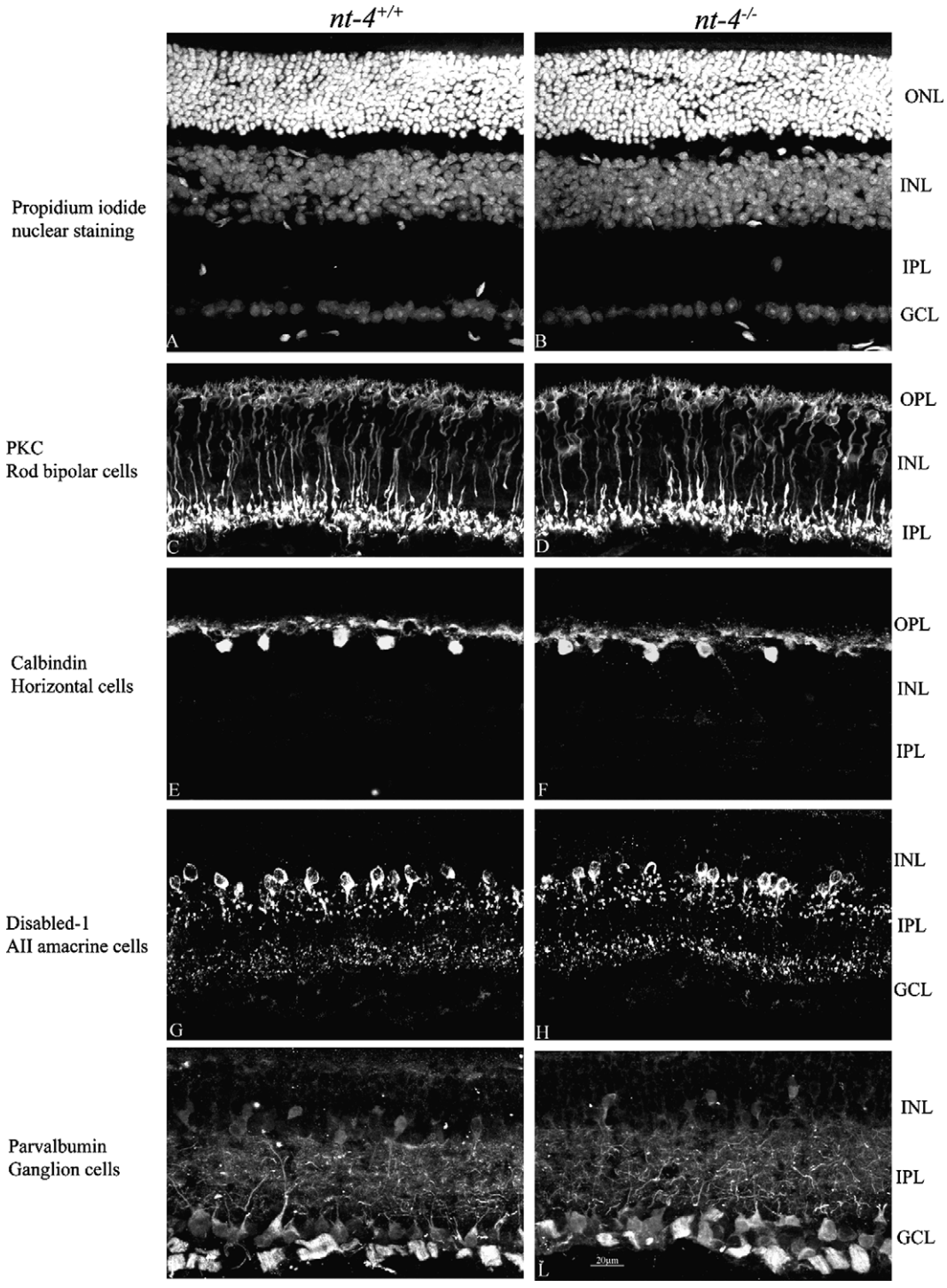

Fig. 8. Immunocytochemistry on retinal sections. Confocal fluorescence photomicrographs of radial sections through mouse retinas that were labelled using different cellular markers. The propidium iodide staining, used to assess the rows of photoreceptor nuclei (A and B), and immunocytochemistry for protein kinase C (C and D), a marker for rod bipolar cells, calbindin (E and F), a marker for horizontal cells, disabled-1 (G and H), a marker for AII amacrine cells, and a parvalbumin (I and L) marker for retinal ganglion cells, did not reveal differences between *nt-4*$^{+/+}$ and *nt-4*$^{-/-}$ mice. Scale bar = 20 μm.

principal metabolite DOPAC in mutant and control mice. We observed a normal content of DA in the retina of *nt*-4$^{-/-}$ mice with an increased turnover of DA, as assessed by measuring the DOPAC/DA ratio. However, whether altered DA turnover stems from a different rate of release at the rings around AII or at non-AII varicosities remains to be investigated. Previous reports (e.g., Iuvone, Galli, Garrison-Gund, & Neff, 1978; Nir et al., 2000) and the present data showed that light stimulates the turnover of DA in the retina without significantly affecting the steady state level of the transmitter. Interestingly, differences of DA turnover between *nt*-4$^{-/-}$ and *nt*-4$^{+/+}$ mice were observed only following

illumination, suggesting that the absence of NT-4 does not affect the amount of basal, unstimulated DA release and/or metabolism. We hypothesize that the increased TH immunopositive processes and varicosities associated with the absence of NT-4 release proportionately higher amounts of DA upon stimulation with light, and that the DA released under these conditions is rapidly metabolized to DOPAC. Thus, deletion of NT-4 induces an alteration of the retinal dopaminergic network with associated changes of stimulated DA turnover in light.

4.1. What is the functional impact of the present data?

The result showing that NT-4 has a role in modulating the complexity of TH immunopositive retinal processes is in line with a large body of experimental evidence showing that neurotrophins control the maturation of neuronal processes in cortical areas and in hippocampus (Croll et al., 1999; Horch, Kruttgen, Portbury, & Katz, 1999; McAllister, Lo, & Katz, 1995; McAllister, Katz, & Lo, 1996; McAllister, Katz, & Lo, 1997; Tolwani et al., 2002; Wirth, Brun, Grabert, Patz, & Wahle, 2003). Specifically in the retina, NT-4 exerts an opposite action to that of BDNF on the TH immunopositive network. Indeed, an exogenous supply of BDNF in developing retina induces an increase of the dopaminergic network (Cellerino et al., 1998) similar to the results found in *nt-4*$^{-/-}$ mice. In particular, intraocular injections of BDNF during postnatal development cause increased TH expression and the density of TH immunopositive varicosities in rat retina. On the other hand, in mice homozygous for a null mutation of the *bdnf* gene, retinal dopaminergic neurons are atrophic and the density of TH positive varicosities is reduced (Cellerino et al., 1998). The possibility that changes in the *nt*-4$^{-/-}$ mice are due to a compensatory up-regulation of BDNF can be excluded since we showed that the BDNF protein level is unchanged.

Opposite actions of different neurotrophins on the same neuronal class have previously been reported. In the developing cortex, BDNF stimulates and NT-3 inhibits the dendritic growth of layer IV pyramidal cells while having the opposite effect on dendritic growth of neurons in layer VI (McAllister et al., 1997). Moreover, the two TrkB receptor ligands, BDNF and NT-4 exert different actions on the development of specific cortical neurons. Indeed, these two neurotrophins influence the dendritic growth of developing visual cortical neurons, but with different laminar specificity (McAllister et al., 1995). In the developing retina, neurite outgrowth of ganglion cells is differentially modulated by BDNF and NT-4 (Bosco & Linden, 1999). In this regard there is increasing evidence for interactive developmental effects between amacrine cells and RGCs and we cannot exclude the possibility that the effects observed on the TH immunopositive amacrine cells in *nt*-4$^{-/-}$ mice are mediated indirectly via some type of cell-cell interaction.

The novelty of our finding is that BDNF and NT-4 can exert *opposite* actions on a defined neuronal population. It is now well-known that binding of BDNF and NT-4 to TrkB activate different intracellular signalling pathways (Minichiello et al., 1998) and that a divergence in TrkB signalling underlies the distinct activities of NT-4 and BDNF (Fan et al., 2000). In particular the mutation of the Shc binding site in the trkB gene revealed distinctive responses to BDNF and NT-4 (Minichiello et al., 1998). The trkB mutation resulted in selective loss of NT-4-sensitive sensory neurons with only a modest effect on BDNF-sensitive neurons. This result and other differential responses to NT-4 and BDNF in the trkB mutants suggest a differential activation of trkB and its associated signalling mechanisms by the two ligands (Minichiello et al., 1998). We extend these previous findings by demonstrating that the divergence of BDNF and NT-4 signalling can lead to antagonistic biological actions, at least in the retina.

The biological significance of having BDNF and NT-4 acting on the same TrkB receptor expressed in dopaminergic amacrine cells is unclear. TrkB expression in dopaminergic cells is a conserved trait of vertebrates (Cellerino & Kohler, 1997). On the other hand, the morphology of dopaminergic plexus is highly variable. Dopaminergic cells form a dense network with processes that stratify in stratum 1 of IPL, but also accessory innervations in stratum 3 and stratum 5, which are variable even within mammals. Even more variable is the extent of axon-like processes ascending towards the outer OPL (Dacey, 1990; Kolb et al., 1990; Kolb, 1997; Voigt & Wassle, 1987). The present and previous (Cellerino et al., 1998) results showed that the absence of single genes, the *nt-4* and *bdnf*, respectively, induce opposite changes in the morphology of dopaminergic amacrine cells and also influence the extent of the ascending processes. We raise the hypothesis that the different levels of expression and opposite actions of BDNF and NT-4 contribute to control the development of structural properties of dopaminergic retinal cells to determine the specific architecture of the different mammalian species.

5. Conclusions

In the present paper we showed that the maturation of dopaminergic retinal circuitry and dopamine turnover during daylight are altered in *nt-4*$^{-/-}$ mice. We suggest that NT-4 controls the maturation of dopaminergic processes and instructs the formation of sites for dopamine release, possibly including the spatial dynamics of varicosity formation and their distribution along processes.

Acknowledgments

We thank Enrica Strettoi and Paul Witkovsky for critical reading of the manuscript and helpful suggestions. L.D. is recipient of FIRB Grant RBAUO15YHM. A.C. is recipient of FIRB Grant RBAVO1A7BT. P.M.I. is the recipient of NIH Grants EY014764 and EY004864.

References

Alsina, B., Vu, T., & Cohen-Cory, S. (2001). Visualizing synapse formation in arborizing optic axons in vivo: dynamics and modulation by BDNF. *Nature Neuroscience, 4*, 1093–1101.

Barbacid, M. (1994). The Trk family of neurotrophin receptors. *Journal of Neurobiology, 25*, 1386–1403.

Bennett, J. L., Zeiler, S. R., & Jones, K. R. (1999). Patterned expression of BDNF and NT-3 in the retina and anterior segment of the developing mammalian eye. *Investigative Ophthalmology and Visual Science, 40*, 2996–3005.

Berkemeier, L. R., Winslow, J. W., Kaplan, D. R., Nikolics, K., Goeddel, D. V., & Rosenthal, A. (1991). Neurotrophin-5: a novel neurotrophic factor that activates trk and trkB. *Neuron, 7*, 857–866.

Bloomfield, S. A., & Dacheux, R. F. (2001). Rod vision: pathways and processing in the mammalian retina. *Progress in Retinal and Eye Research, 20*, 351–384.

Bosco, A., & Linden, R. (1999). BDNF and NT-4 differentially modulate neurite outgrowth in developing retinal ganglion cells. *Journal of Neuroscience Research, 57*, 759–769.

Cellerino, A., Arango-Gonzalez, B., Pinzon-Duarte, G., & Kohler, K. (2003). Brain-derived neurotrophic factor regulates expression of vasoactive intestinal polypeptide in retinal amacrine cells. *Journal Comparative Neurology, 467*, 97–104.

Cellerino, A., Carroll, P., Thoenen, H., & Barde, Y. A. (1997). Reduced size of retinal ganglion cell axons and hypomyelination in mice lacking brain-derived neurotrophic factor. *Molecular and Cellular Neuroscience, 9*, 397–408.

Cellerino, A., & Kohler, K. (1997). Brain-derived neurotrophic factor/neurotrophin-4 receptor TrkB is localized on ganglion cells and dopaminergic amacrine cells in the vertebrate retina. *Journal Comparative Neurology, 386*, 149–160.

Cellerino, A., Pinzon-Duarte, G., Carroll, P., & Kohler, K. (1998). Brain-derived neurotrophic factor modulates the development of the dopaminergic network in the rodent retina. *Journal of Neuroscience, 18*, 3351–3362.

Chytrova, G., & Johnson, J. E. (2004). Spontaneous retinal activity modulates BDNF trafficking in the developing chick visual system. *Molecular and Cellular Neuroscience, 25*, 549–557.

Cohen, A., Bray, G. M., & Aguayo, A. J. (1994). Neurotrophin-4/5 (NT-4/5) increases adult rat retinal ganglion cell survival and neurite outgrowth in vitro. *Journal of Neurobiology, 25*, 953–959.

Cohen-Cory, S., & Fraser, S. E. (1995). Effects of brain-derived neurotrophic factor on optic axon branching and remodelling in vivo. *Nature, 378*, 192–196.

Conover, J. C., Erickson, J. T., Katz, D. M., Bianchi, L. M., Poueymirou, W. T., McClain, J., et al. (1995). Neuronal deficits, not involving motor neurons, in mice lacking BDNF and/or NT4. *Nature, 375*, 235–238.

Croll, S. D., Suri, C., Compton, D. L., Simmons, M. V., Yancopoulos, G. D., Lindsay, R. M., et al. (1999). Brain-derived neurotrophic factor null mutant mice exhibit passive avoidance deficits, increased seizure severity and in vitro hyperexcitability in the hippocampus and entorhinal cortex. *Neuroscience, 93*, 1491–1506.

Cui, Q., & Harvey, A. R. (1994). NT-4/5 reduces naturally occurring retinal ganglion cell death in neonatal rats. *Neuroreport, 5*, 1882–1884.

Cui, Q., & Harvey, A. R. (1995). At least two mechanisms are involved in the death of retinal ganglion cells following target ablation in neonatal rats. *Journal of Neuroscience, 15*, 8143–8155.

Cui, Q., & Harvey, A. R. (2000). NT-4/5 reduces cell death in inner nuclear as well as ganglion cell layers in neonatal rat retina. *Neuroreport, 11*, 3921–3924.

Dacey, D. M. (1990). The dopaminergic amacrine cell. *Journal of Comparative Neurology, 301*, 461–489.

Di Polo, A., Cheng, L., Bray, G. M., & Aguayo, A. J. (2000). Colocalization of TrkB and brain-derived neurotrophic factor proteins in green-red-sensitive cone outer segments. *Investigative Ophthalmology and Visual Science, 41*, 4014–4021.

Du, J. L., & Poo, M. M. (2004). Rapid BDNF-induced retrograde synaptic modification in a developing retinotectal system. *Nature, 429*, 878–883.

Erickson, J. T., Conover, J. C., Borday, V., Champagnat, J., Barbacid, M., Yancopoulos, G., et al. (1996). Mice lacking brain-derived neurotrophic factor exhibit visceral sensory neuron losses distinct from mice lacking NT4 and display a severe developmental deficit in control of breathing. *Journal of Neuroscience, 16*, 5361–5371.

Famiglietti, E. V., & Kolb, H. (1975). A bistratified amacrine cell and synaptic cirucitry in the inner plexiform layer of the retina. *Brain Research, 84*, 293–300.

Fan, G., Egles, C., Sun, Y., Minichiello, L., Renger, J. J., Klein, R., et al. (2000). Knocking the NT4 gene into the BDNF locus rescues BDNF deficient mice and reveals distinct NT4 and BDNF activities. *Nature Neuroscience, 3*, 350–357.

Fox, E. A., Phillips, R. J., Baronowsky, E. A., Byerly, M. S., Jones, S., & Powley, T. L. (2001). Neurotrophin-4 deficient mice have a loss of vagal intraganglionic mechanoreceptors from the small intestine and a disruption of short-term satiety. *Journal of Neuroscience, 21*, 8602–8615.

Frost, D. O. (2001). BDNF/trkB signaling in the developmental sculpting of visual connections. *Progress in Brain Research, 134*, 35–49.

Hallbook, F., Backstrom, A., Kullander, K., Ebendal, T., & Carri, N. G. (1996). Expression of neurotrophins and trk receptors in the avian retina. *Journal Comparative Neurolology, 364*, 664–676.

Hallbook, F., Ibanez, C. F., & Persson, H. (1991). Evolutionary studies of the nerve growth factor family reveal a novel member abundantly expressed in Xenopus ovary. *Neuron, 6*, 845–858.

Herzog, K. H., Bailey, K., & Barde, Y. A. (1994). Expression of the BDNF gene in the developing visual system of the chick. *Development, 120*, 1643–1649.

Herzog, K. H., & von Bartheld, C. S. (1998). Contributions of the optic tectum and the retina as sources of brain-derived neurotrophic factor for retinal ganglion cells in the chick embryo. *Journal of Neuroscience, 18*, 2891–2906.

Horch, H. W., Kruttgen, A., Portbury, S. D., & Katz, L. C. (1999). Destabilization of cortical dendrites and spines by BDNF. *Neuron, 23*, 353–364.

Isenmann, S., Cellerino, A., Gravel, C., & Bahr, M. (1999). Excess target-derived brain-derived neurotrophic factor preserves the transient uncrossed retinal projection to the superior colliculus. *Molecular Cell Neuroscience, 14*, 52–65.

Iuvone, P. M. (1986). Neurotransmitters and neuromodulators in the retina: regulation, interactions and cellular effects. In R. Adler & D. Farber (Eds.), *The retina, a model for cell biology studies, part II* (pp. 1–72). Orlando: Academic Press.

Iuvone, P. M., Galli, C. L., Garrison-Gund, C. K., & Neff, N. H. (1978). Light stimulates tyrosine hydroxylase activity and dopamine synthesis in retinal amacrine neurons. *Science, 202*, 902–910.

Jelsma, T. N., Friedman, H. H., Berkelaar, M., Bray, G. M., & Aguayo, A. J. (1993). Different forms of the neurotrophin receptor trkB mRNA predominate in rat retina and optic nerve. *Journal of Neurobiology, 24*, 1207–1214.

Karlsson, M., & Hallbook, F. (1998). Kainic acid, tetrodotoxin and light modulate expression of brain-derived neurotrophic factor in developing avian retinal ganglion cells and their tectal target. *Neuroscience, 83*, 137–150.

Kim, T. J., & Jeon, C. J. (2006). Morphological classification of parvalbumin-containing retinal ganglion cells in mouse: single-cell injection after immunocytochemistry. *Investigative Ophthalmology and Visual Science, 47*, 2757–2764.

Kolb, H. (1997). Amacrine cells of mammalian retina: neurocircuitry and functional roles. *Eye, 11*, 904–923.

Kolb, H., Cuenca, N., Wang, H. H., & Dekorver, L. (1990). The synaptic organization of the dopaminergic amacrine cell in the cat retina. *Journal of Neurocytology, 19*, 343–366.

Liu, X., Ernfors, P., Wu, H., & Jaenisch, R. (1995). Sensory but not motor neuron deficits in mice lacking NT4 and BDNF. *Nature, 375*, 238–241.

Lom, B., Cogen, J., Sanchez, A. L., Vu, T., & Cohen-Cory, S. (2002). Local and target-derived brain-derived neurotrophic factor exert opposing effects on the dendritic arborization of retinal ganglion cells in vivo. *Journal of Neuroscience, 22*, 7639–7649.

Lowry, O. H., Rosebrough, N. J., Farr, A. L., & Randall, R. J. (1951). Protein measurement with the folin phenol reagent. *Journal of Biological Chemistry, 193*, 265–275.

Lucas, G., Hendolin, P., Harkany, T., Agerman, K., Paratcha, G., Holmgren, C., et al. (2003). Neurotrophin-4 mediated TrkB activation reinforces morphine-induced analgesia. *Nature Neuroscience, 6*, 221–222.

McAllister, A. K., Katz, L. C., & Lo, D. C. (1996). Neurotrophin regulation of cortical dendritic growth requires activity. *Neuron, 17*, 1057–1064.

McAllister, A. K., Katz, L. C., & Lo, D. C. (1997). Opposing roles for endogenous BDNF and NT-3 in regulating cortical dendritic growth. *Neuron, 18*, 767–778.

McAllister, A. K., Lo, D. C., & Katz, L. C. (1995). Neurotrophins regulate dendritic growth in developing visual cortex. *Neuron, 15*, 791–803.

Menna, E., Cenni, M. C., Naska, S., & Maffei, L. (2003). The anterogradely transported BDNF promotes retinal axon remodeling during eye specific segregation within the LGN. *Molecular and Cellular Neuroscience, 24*, 972–983.

Minichiello, L., Casagranda, F., Tatche, R. S., Stucky, C. L., Postigo, A., Lewin, G. R., et al. (1998). Point mutation in trkB causes loss of NT4-dependent neurons without major effects on diverse BDNF responses. *Neuron, 21*, 335–345.

Neal, M., Cunningham, J., Lever, I., Pezet, S., & Malcangio, M. (2003). Mechanism by which brain-derived neurotrophic factor increases dopamine release from the rabbit retina. *Investigative Ophthalmology and Visual Science, 44*, 791–798.

Nir, I., Haque, R., & Iuvone, P. M. (2000). Diurnal metabolism of dopamine in the mouse retina. *Brain Research, 870*(1–2), 118–125.

Pattabiraman, P. P., Tropea, D., Chiaruttini, C., Tongiorgi, E., Cattaneo, A., & Domenici, L. (2005). Neuronal activity regulates the developmental expression and subcellular localization of cortical BDNF mRNA-isoforms in vivo. *Molecular and Cellular Neuroscience, 28*, 556–570.

Perez, M. T., & Caminos, E. (1995). Expression of brain-derived neurotrophic factor and of its functional receptor in neonatal and adult rat retina. *Neuroscience Letters, 183*, 96–99.

Pignatelli, V., Cepko, C. L., & Strettoi, E. (2004). Inner retinal abnormalities in a mouse model of Leber's congenital amaurosis. *Journal of Comparative Neurology, 469*, 351–359.

Pignatelli, V., & Strettoi, E. (2004). Bipolar cells of the mouse retina: a gene gun, morphological study. *Journal of Comparative Neurology, 476*, 254–266.

Pinzon-Duarte, G., Arango-Gonzalez, B., Guenther, E., & Kohler, K. (2004). Effects of brain-derived neurotrophic factor on cell survival, differentiation and patterning of neuronal connections and Muller glia cells in the developing retina. *European Journal of Neuroscience, 19*, 1475–1484.

Pollock, G. S., & Frost, D. O. (2003). Complexity in the modulation of neurotrophic factor mRNA expression by early visual experience. *Brain Research Developmental Brain Research, 143*, 225–232.

Pollock, G. S., Robichon, R., Boyd, K. A., Kerkel, K. A., Kramer, M., Lyles, J., et al. (2003). TrkB receptor signalling regulates developmental death dynamics, but not final number, of retinal ganglion cells. *Journal of Neuroscience, 23*, 10137–10145.

Rickman, D. W. (2000). Neurotrophins and development of the rod pathway: an elementary deduction. *Microscopy Research and Technique, 50*, 124–129.

Rohrer, B., Korenbrot, J. I., LaVail, M. M., Reichardt, L. F., & Xu, B. (1999). Role of neurotrophin receptor TrkB in the maturation of rod photoreceptors and establishment of synaptic transmission to the inner retina. *Journal of Neuroscience, 19*, 8919–8930.

Rohrer, B., LaVail, M. M., Jones, K. R., & Reichardt, L. F. (2001). Neurotrophin receptor TrkB activation is not required for the postnatal survival of retinal ganglion cells in vivo. *Experimental Neurology, 172*, 81–91.

Roosen, A., Schober, A., Strelau, J., Bottner, M., Faulhaber, J., Bendner, G., et al. (2001). Lack of neurotrophin-4 causes selective structural and chemical deficits in sympathetic ganglia and their preganglionic innervation. *Journal of Neuroscience, 21*, 3073–3084.

Rothe, T., Bahring, R., Carroll, P., & Grantyn, R. (1999). Repetitive firing deficits and reduced sodium current density in retinal ganglion cells developing in the absence of BDNF. *Journal of Neurobiology, 40*, 407–419.

Sawai, H., Clarke, D. B., Kittlerova, P., Bray, G. M., & Aguayo, A. J. (1996). Brain-derived neurotrophic factor and neurotrophin-4/5 stimulate growth of axonal branches from regenerating retinal ganglion cells. *Journal of Neuroscience, 16*, 3887–3894.

Seki, M., Nawa, H., Fukuchi, T., Abe, H., & Takei, N. (2003). BDNF is upregulated by postnatal development and visual experience: quantitative and immunohistochemical analyses of BDNF in the rat retina. *Investigative Ophthalmology and Visual Science, 44*, 3211–3218.

Seki, M., Tanaka, T., Nawa, H., Usui, T., Fukuchi, T., Ikeda, K., et al. (2004). Involvement of brain-derived neurotrophic factor in early retinal neuropathy of streptozotocin-induced diabetes in rats: therapeutic potential of brain-derived neurotrophic factor for dopaminergic amacrine cells. *Diabetes, 53*, 2412–2419.

Smith, D. J., Leil, T. A., & Liu, X. (2003). Neurotrophin-4 is required for tolerance to morphine in the mouse. *Neuroscience Letters, 340*, 103–106.

Spalding, K. L., Cui, Q., & Harvey, A. R. (1998). The effects of central administration of neurotrophins or transplants of fetal tectal tissue on retinal ganglion cell survival following removal of the superior colliculus in neonatal rats. *Brain Research Developmental Brain Research, 107*, 133–142.

Spalding, K. L., Cui, Q., & Harvey, A. R. (2005). Retinal ganglion cell neurotrophin receptor levels and trophic requirements following target ablation in the neonatal rat. *Neuroscience, 131*, 387–395.

Stucky, C. L., Shin, J. B., & Lewin, G. R. (2002). Neurotrophin-4: a survival factor for adult sensory neurons. *Current Biology, 12*, 1401–1404.

Timmusk, T., Belluardo, N., Metsis, M., & Persson, H. (1993). Widespread and developmentally regulated expression of neurotrophin-4 mRNA in rat brain and peripheral tissues. *European Journal of Neuroscience, 5*, 605–613.

Tolwani, R. J., Buckmaster, P. S., Varma, S., Cosgaya, J. M., Wu, Y., Suri, C., et al. (2002). BDNF overexpression increases dendrite complexity in hippocampal dentate gyrus. *Neuroscience, 114*, 795–805.

Tongiorgi, E., Righi, M., & Cattaneo, A. (1998). A non-radioactive in situ method that does not require RNAse-free conditions. *Journal of Neuroscience Methods, 85*, 129–139.

Tork, I., & Stone, J. (1979). Morphology of catecholamine-containing amacrine cells in the cat's retina, as seen in retinal whole mounts. *Brain Research, 169*, 261–273.

Voigt, T., & Wassle, H. (1987). Dopaminergic innervation of AII amacrine cells in mammalian retina. *Journal of Neuroscience, 7*, 4115–4128.

von Bartheld, C. S. (1998). Neurotrophins in the developing and regenerating visual system. *Histology and Histopathology, 13*, 437–459.

Wahlin, K. J., Campochiaro, P. A., Zack, D. J., & Adler, R. (2000). Neurotrophic factors cause activation of intracellular signaling pathways in Muller cells and other cells of the inner retina, but not photoreceptors. *Investigative Ophthalmology and Visual Science, 41*, 927–936.

Wexler, E. M., Berkovich, O., & Nawy, S. (1998). Role of the low-affinity NGF receptor (p75) in survival of retinal bipolar cells. *Visual Neuroscience, 15*, 211–218.

Wirth, M. J., Brun, A., Grabert, J., Patz, S., & Wahle, P. (2003). Accelerated dendritic development of rat cortical pyramidal cells and interneurons after biolistic transfection with BDNF and NT4/5. *Development, 130*, 5827–5838.

Witkovsky, P. (2004). Dopamine and retinal function. *Documenta Ophthalmologica, 108*, 17–40.

Witkovsky, P., Arango-Gonzalez, B., Haycock, J. W., & Kohler, K. (2005). Rat retinal dopaminergic neurons: differential maturation of somatodendritic and axonal compartments. *Journal of Comparative Neurology, 481*, 352–362.

Witkovsky, P., Veisenberger, E., Haycock, J. W., Akopian, A., Garcia-Espana, A., & Meller, E. (2004). Activity-dependent phosphorylation of tyrosine hydroxylase in dopaminergic neurons of the rat retina. *Journal of Neuroscience, 24*, 4242–4249.

Wulle, I., & Schnitzer, J. (1989). Distribution and morphology of tyrosine hydroxylase-immunoreactive neurons in the developing mouse retina. *Brain Research Developmental Brain Research, 48*, 59–72.

Xie, C. W., Sayah, D., Chen, Q. S., Wei, W. Z., Smith, D., & Liu, X. (2000). Deficient long-term memory and long-lasting long-term potentiation in mice with a targeted deletion of neurotrophin-4 gene. *Proceedings of the National Academy of Sciences of the United States of America, 97*, 8116–8121.